Geochemical Journal, Vol. 48, pp. 309 to 320, 2014 doi:10.2343/geochemj.2.0307

Microanalysis of Pb isotope ratios of low-Pb glass samples by femtosecond laser ablation-multiple ion counter-ICP-mass spectrometry (fsLA-MIC-ICP-MS)

QING CHANG,[1]* JUN-ICHI KIMURA,[1] TAKASHI MIYAZAKI,[1] SATOSHI SASAKI[2] and NOBUYUKI KANAZAWA[2]

[1]Institute for Research on Earth Evolution, Japan Agency for Marine-Earth Science and Technology, 2-15 Natsushima-cho, Yokosuka 237-0061, Japan
[2]ThermoFisher Scientific K.K., 3-9 Moriya-cho, Yokohama 221-0022, Japan

(*Received October 22, 2013; Accepted February 19, 2014*)

We report high-resolution *in situ* Pb isotope analysis ($^{207}Pb/^{206}Pb$ and $^{208}Pb/^{206}Pb$ ratios) by femtosecond laser ablation-multiple ion counter-inductively coupled plasma-mass spectrometry (fsLA-MIC-ICP-MS) for low-Pb geological reference glasses. Pb isotope analysis was realized using a multiple ion counter (MIC) and a modified inductively coupled plasma (ICP) ion interface to improve the signal-to-noise ratio and instrumental sensitivity, respectively. Use of femtosecond deep-UV (200 nm) laser ablation enhanced the sampling efficiency of the small amount of glass. Pb memory from sample-skimmer cones were subtracted using an on-peak background method. Instrumental mass bias correction and inter-MIC calibration were performed simultaneously using a standard-sample bracketing method. The optimized analytical protocol was applied to various rock reference glasses (BHVO-2G, BCR-2G and GSD-1G from the United States Geological Survey, and the MPI-DING series glasses: KL2-G, StHs6/80-G, ATHO-G, T1-G, and GOR132-G from the Max Plank Institute for Chemistry, Germany) with spatial resolution of ~30-μm diameter and 3–25-μm depth. The accuracy achieved was better than 0.38% compared with reference values, and the reproducibility was better than 1.0% (2SD) for both $^{207}Pb/^{206}Pb$ and $^{208}Pb/^{206}Pb$ ratios from the glasses with Pb concentrations of 1.7–19 ppm. We found that proper control of signal intensity is crucial for accurate and precise isotopic ratio measurements by the miniature MIC. Signal intensity higher than 300 kcps results in instantaneous saturation of the MIC and consequent inaccurate isotopic ratio measurements. The optimization of the fsLA-MIC-ICP-MS system allows high-throughput Pb isotopic microanalysis with the precision, accuracy and lateral spatial resolution comparable to those of secondary ion mass spectrometry, indicating the versatility of this method for *in-situ* microanalysis of Pb isotopes in the geosciences.

Keywords: Pb isotopes, laser ablation, ICP-MS, multiple ion counting (MIC), silicate glass geological reference materials

INTRODUCTION

In situ analysis of Pb isotopes by laser ablation coupled with multiple-collector inductively coupled plasma mass spectrometry (LA-MC-ICP-MS) has been applied to a wide variety of geological samples, including silicate minerals, glasses and melt inclusions (Mathez and Waight, 2003; Peate *et al*., 2003; Gagnevin *et al*., 2005; Kent and Dilles, 2005; Paul *et al*., 2005; Simon *et al*., 2007; Kent, 2008a, b; Paul *et al*., 2011; Westgate *et al*., 2011; Kimura *et al*., 2013). For Pb-rich material and/or when a large ablation spot is possible, LA-MC-ICP-MS using Faraday collectors can provide *in situ* Pb isotope analysis with accuracy of several per mil, even for the minor ^{204}Pb (cf., Kimura *et al*., 2013). However, it has not been possible to apply this technique to low-Pb materials, such as silicate glass and magmatic melt inclusions, especially for analyses where high spatial resolution is desired.

High spatial resolution capability, for instance, down to 20–30-μm diameter, is required in applications of olivine melt inclusion analysis (e.g., Saal *et al*. (2005) by secondary ion mass spectrometry (SIMS), and Paul *et al*. (2011) by LA-MC-ICP-MS). The incorporation of ion counters (ICs) into mass spectrometry is a recent advancement that extends LA-MC-ICP-MS for Pb isotope analysis, because analysis with an extremely small ion beam is commonly required owing to the restrictions of small sampling volume and low Pb content (e.g., <10 ppm). In many previous studies, one to a few ICs have been combined with Faraday collectors (FCs). However, only minor isotope ^{204}Pb and interfering mercury signals were usually monitored by the ICs, while the major isotopes of Pb ($^{206,207,208}Pb$) and $^{203,205}Tl$ (for mass bias correction) were measured by the FCs (e.g., Kent and Dilles, 2005; Paul *et al*., 2011). When different types of detectors are employed, their cross calibration is crucial for a precise and accu-

*Corresponding author (e-mail: qchang@jamstec.go.jp)

rate isotopic ratio analysis (e.g., Kent and Dilles, 2005). The linearity difference between the ICs and FCs is also an essential factor directly affecting the results.

The most significant advantage of MIC analysis over single IC analysis is (1) a lower counting statistic error due to longer signal integration for each isotope and (2) cancellation of flicker signal noise from the ICP plasma by simultaneous counting of the isotopes. Souders and Sylvester (2008) demonstrated *in situ* Pb isotope analysis of silicate glasses with an IC array, also termed multiple ion counters (MICs). They showed that $^{207,208}Pb/^{206}Pb$ ratios could be measured with an accuracy of 0.45% with reproducibility of <0.5% relative standard deviations (2SDs) for samples with ~2 ppm Pb using an ablation spot of 40–69-μm. However, their ^{204}Pb-based isotope ratios were inferior in precision and accuracy, although they corrected for ^{204}Hg interference on ^{204}Pb by monitoring ^{202}Hg concurrently using ICs. This is always true for LA-MC-ICP-MS because large interference from ^{204}Hg on minor ^{204}Pb in low-Pb samples is inevitable (Kent and Dilles, 2005; Paul *et al*., 2011).

In this work, we demonstrate that laser ablation-multiple ion counter-inductively coupled plasma-mass spectrometry (LA-MIC-ICP-MS) is a simple and rapid method for *in situ* determination of Pb isotope ratios of $^{207,208}Pb/^{206}Pb$ from low-Pb (1.7–19 ppm) geological glasses at high spatial resolution of ~30-μm diameter. We tested Pb isotopic analyses of reference glasses using a deep-UV (200 nm wavelength) femtosecond laser ablation system (fsLA) (Kimura and Chang, 2012) connected with MIC-ICP-MS. Instrumental mass bias and inter-MIC calibration were corrected through a standard-sample bracketing method (Albarède *et al*., 2004) and baseline subtraction performed by on-peak background measurement before laser firing (e.g., Kimura *et al*., 2013).

Samples

The USGS geological rock reference glasses (BHVO-2G and GSD-1G) and MPI-DING glasses (KL2-G, StHs6/80-G, ATHO-G, T1-G, and GOR132-G) were analyzed. These glasses have low-Pb concentrations ranging from 1.7 to 19.5 ppm (GeoReM, http://georem.mpch-mainz.gwdg.de, Application Ver. 15, 2013; Jochum *et al*., 2005a, 2006) except for GSD-1G, which was doped with selected rare earth elements and transition metals including Pb (48 ppm, Guillong *et al*., 2005). These reference glasses have been well characterized for Pb isotopes (Elburg *et al*., 2005; Jochum *et al*., 2005b, 2011; Paul *et al*., 2005) and therefore, were suitable for validating the analytical method. The selected USGS glasses were all basaltic in composition, whereas the MPI-DING glasses covered a wide range of compositions: basalt (KL2-G), andesite (StHs6/80-G), rhyolite (ATHO-G), quartz-diorite (T1-G), and komatiite (GOR132-G). Jochum *et al*. (2005b) noted Pb contamination during glass preparation and the heterogeneity of the MPI-DING glasses. However, the influence of these deficiencies is less significant considering the precision obtained from the micro-analytical techniques, whereas it does affect a high precision analysis with thermal ionization mass spectrometry (TIMS) and solution MC-ICP-MS.

We used BCR-2G (11.0 ppm Pb, GeoReM) and NIST SRM 612 (38.96 ppm Pb, Pearce *et al*., 1997) as primary bracketing standards. Both have moderate Pb content and can generate sufficient signal intensity but not saturate the ICs in our routine LA condition. Pb isotopic ratios are taken from solution MC-ICP-MS analyses for BCR-2G (Elburg *et al*., 2005) and from double-spike solution MC-ICP-MS for NIST SRM 612 (Baker *et al*., 2004). BCR-2G and NIST SRM 612 have very different chemical and physical properties. BCR-2G is an opaque basalt glass, whereas NIST SRM 612 is a transparent synthetic glass with a rhyolite-like composition. The difference was supposed to affect laser coupling with the materials ablated. However, no significant matrix effect was observed in our fsLA-MIC-ICP-MS data (see below).

Instrumentation

In situ Pb isotope analyses were performed on a double focusing MIC-ICP-MS (Thermo Fisher Scientific, Neptune, Bremen, Germany) fitted with a 200/266 nm fsLA system, housed at the Institute for Research on Earth Evolution (IFREE), Japan Agency of Marine-Earth Science and Technology (JAMSTEC). The fsLA system and the MIC-ICP-MS used here have been described in detail elsewhere (Kimura *et al*., 2011, 2013; Kimura and Chang, 2012) and brief descriptions of the instrumental setup for this work are listed in Supplementary Table S1. The important details for this work are given below.

Instrumental sensitivity, detecting efficiency and signal-to-noise ratio (S/N) are critical in controlling the quality of Pb isotope measurements under total Pb intensity below 10 mV (Sounders and Sylvester, 2008). This is particularly true for analysis of low-Pb at high spatial resolution by LA-ICP-MS. To improve the S/N and detecting efficiency, we used MICs instead of FCs to collect all Pb isotopes. Eight miniature Channeltron-type ICs were installed on our MC-ICP-MS, of which four were attached to the low-mass Faraday cup side (L4) and spaced specifically to collect all Pb isotopes ($^{204,206,207,208}Pb$) simultaneously. Plateau voltages and yields of all ICs involved were optimized and checked periodically using solution mode through an Aridus II desolvating nebulizer (CETAC Technologies, Omaha, Nebraska, USA) to deliver a stable Pb beam (~10 kcps of ^{208}Pb). Yield calibration of MICs can be determined by sequentially intro-

ducing the same ^{208}Pb signal to each IC, but was less precise because of transient nature of MICs. We observed that the counting efficiency dropped 2–4% for IC2 and IC3, which collected ^{206}Pb and ^{207}Pb, respectively (Table S1), and slightly large, 3–7% for IC4, which collected ^{208}Pb in 30 minutes. The decay of ICs is quite rapid and differs between isotopes dependent on signal intensities. This prevents use of inter-MIC calibrations as for large ICs (e.g., full size SEM) (Kimura *et al*., 2011). Therefore we did not perform inter-MIC calibration. Dark noise correction, which usually was below 0.01 cps, was done with the analytical valve of Neptune closed to shutdown ions from plasma ion source. A dead time correction was applied with a default value of 70 ns for all ICs.

We tested several possible ways to improve instrumental sensitivity, including the addition of a large extra rotary pump (E2M80, Edwards, West Sussex, UK) connected in parallel with the original interface pump, and the use of high performance (X-) skimmer and JET-sample cones (Bouman *et al*., 2008). Sensitivity was increased by about 10 times using this interface setting. These modifications on the plasma interface did not cause any significant alteration of mass fractionation factors between Pb isotopes (Kimura *et al*., 2013), although large but stable instrumental mass bias was present due to mass fractionation that occurred at the ICP interface (Hirata, 1996). The stable mass fractionation at the interface allowed for the application of the standard bracketing method (see below). Therefore, X-skimmer and JET-sample cones, which gave the highest sensitivity, were used in most of the analytical sessions in this work. Nevertheless, X-skimmer and Normal (N) sample cones were also tested for comparison. Typical sensitivity of 18–23 kilo counts per second (kcps) of total Pb intensity per ppm Pb, at 5 Hz LA repetition on BCR-2G (11.0 ppm Pb) with ~30-μm crater, was achieved by the X-JET combination.

The fsLA system used in this work provides a 266- or 200-nm laser beam from the 3rd or 4th harmonic waves of the fundamental 800-nm fs-laser (Kimura and Chang, 2012). Considering ablation features and the small sample volume desired for this work, we only used the 200-nm laser beam. Ablation was performed using a helium carrier gas in a small-volume ablation cell (~20 cm^3 internal volume) with parallel inlet nozzles for the helium flow (Kimura and Chang, 2012). Pulse duration of the fsLA was assumed to be < 300 fs. Total laser energy prior to the shaping aperture was ~40 μJ. The laser fluence on the sample surface was ~6 J cm^{-2} (Kimura and Chang, 2012). Femtosecond laser ablation is believed to have less thermal effect and cause less damage at the ablation site and consequently, suppresses elemental fractionation (e.g., Kimura and Chang, 2012). Moreover, efficient sample aerosol transfer to the ICP, about two times better than

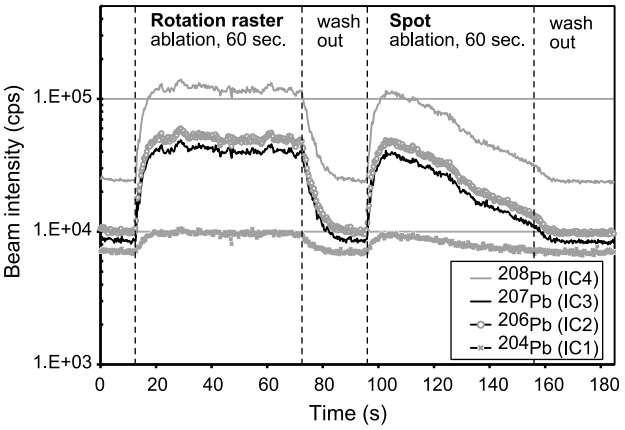

Fig. 1. Comparison of 60-second signal profiles of Pb isotopes generated from rotation raster (see text) and spot ablation on BCR-2G by 200-nm femto-second laser at 3 Hz laser repetition rate. Rotation raster clearly shows superior signal stability. Resulting crater size is 30 μm for rotation raster and 20 μm for spot ablation. Number in parentheses of legend indicates ion counter (IC) number used to collect designed Pb isotope.

that in 193 nm nanosecond excimer LA, is beneficial for microanalysis (Kimura and Chang, 2012). Ablated sample aerosols were transferred by He gas flow into a 150 mL inner volume PFA buffer chamber, where Ar make-up gas was mixed and injected together into the ICP.

Analytical Protocols

We used a rotation raster protocol (Kimura and Chang, 2012) to lessen downhole elemental fractionation during laser ablation (Kimura *et al*., 2011) and to obtain stable ion beams (Fig. 1). A computer-controlled stage, on which the ablation cell is mounted, rotates under the laser beam at a given radius and travelling speed to fit the desired crater size and ablation duration. The theoretical crater size resulting from this LA mode will be the sum of sizes of the laser beam and stage rotation circle. Under our routine operation conditions, an ablation spot of approximately 30 μm was produced by rotating the sample repeatedly along the circumference of a 3-μm radius circle at 2 μm/s, and by using a laser beam with 20-μm diameter.

The resulted size of the ablated spot varied slightly depending on the composition of the glass, presumably due to laser absorption features of the materials (Czas *et al*., 2012). Crater diameters were consistently smaller on the NIST SRM 612 (soda-lime glass, ~28 μm), but larger on the T1-G (quartz-diorite, 38–40 μm), whereas craters of ~30 μm were normally produced on other basalt, andesite, rhyolite, and komatiite glasses. All analyses in this study were performed using this rotation raster pro-

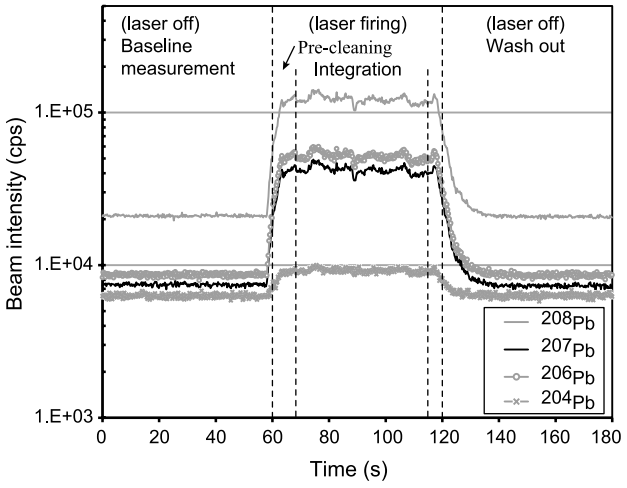

Fig. 2. Time-resolving signal profile in one measurement run of Pb isotopes by fsLA-MIC-ICP-MS. Baseline is taken on peak with laser-off, but with all gases flowing. After 8 s of pre-ablation cleaning with laser firing, sample signal integration starts and continues for ~47 s (180 scans at 0.262 s/scan). 60 s after laser-off allowed washing out sample signals and return to gas blank levels.

tocol. Therefore, the spatial resolution in our Pb isotope analysis was fixed at 30 μm for most of the glasses, which was almost half that of the previous study by Sounders and Sylvester (2008).

Pb signal intensity was adjusted by changing the repetition rate of the laser pulse between 1 and 10 Hz. We measured that the drilling rate was 0.04 μm per shot on basalt glasses. Thus, a 60 s ablation used here (described in following paragraph) resulted in craters with depths of 3–25 μm. This drilling rate allowed normal petrological thin sections (typically 30–40 μm thick) to be analyzed.

We employed an on-peak background subtraction with standard-bracketing method. Pb isotope data were acquired continuously in a static mode for 180 s in one analytical run with ~0.262 s integration time per scan for both standards and unknowns (Fig. 2). Two 30-s baseline measurements were made first in each run before laser firing (Fig. 2). The Pb isotope signals of either standards or unknowns were measured from ~47 s (180 scans at 0.262 s/scan) LA signals after laser-on and stabilization of the Pb signals (Fig. 2). Aerosols from previous measurements may have been deposited as a thin layer on the sample surface. Therefore, to avoid surface contamination, data acquired within ~8 s after laser firing were discarded (pre-ablation; Fig. 2). One-minute washout was used after LA, but it was clear that 10–20 s was sufficient to wash the Pb sample signals to the gas blank levels (Fig. 2). Outlier isotope ratios were removed online with the 2σ outlier test of the Neptune operating software. One measurement run, including baseline measurement, pre-ablation, signal acquisition, washout, and data processing for off-line calculation, took about three minutes.

As shown in Figs. 2 and 1, although ^{204}Pb was collected, its S/N is too bad for quantitation, typically 0.13–0.15 when adjusting ^{208}Pb to suitable level (discussed in later section). Poor S/N is due to low abundance of ^{204}Pb compared to the other Pb isotopes and the high background signal of mass 204, which usually is 6–10 kcps, almost 10 times higher than those of ^{206,207,208}Pb. The high background of mass 204 was contributed mainly by mercury from Ar and helium gases. We have tried to install activated charcoal and duster filters before make-up Ar gas to remove Hg. Two thirds of Hg signal was cut by the filters, but still crucially high for isotope ratio analyses. Furthermore, large amount of carbon was introduced into plasma by using charcoal filter, which may cause problems by depositing on sampling cone and increasing potential contamination. The S/N ratio of ^{204}Pb can be improved to some extent by increasing the size of LA spot. Jochum *et al*. (2005b) used 120 μm LA spot and obtained ^{206,207,208}Pb/^{204}Pb ratios with precisions of 0.3–2% (RSE) for NIST 612 and MPI-DING glasses. However, increasing LA spot will deviate from the main purpose of this study. Therefore, the measured ^{206,207,208}Pb/^{204}Pb ratios in this work were highly variable and erroneous. We reported only ^{207}Pb/^{206}Pb and ^{208}Pb/^{206}Pb here for the measured reference glasses.

The standard was analyzed before and after each sample, because the counting efficiency of the miniature MICs decayed very quickly during the analyses as mentioned in previous section, and considering that bracketing standard and unknown should be measured with as similar conditions as possible.

For the reference glasses, which are presumed to be homogeneous, final Pb isotope ratios were usually derived by an average of multiple spots (e.g., the average of three spots following Jochum *et al*., 2005c). Analytical precision appears improved by the statistical treatment of the data from three spots, but this method is not always applicable for the analysis of melt inclusions where sampling area is limited. In this paper, Pb isotope data based on individual spot analysis are assessed throughout.

Results and Discussion

Effect of Pb beam intensity on isotope ratios

The response of the miniature MICs to varying ion beam intensity has been of great concern for isotope analyses. It has been advisable to match the beam intensities between unknowns and bracketing standards (Sounders and Sylvester, 2008; Nozaki *et al*., 2012; Kimura *et al*., 2013). To examine the linearity of the MICs and finally,

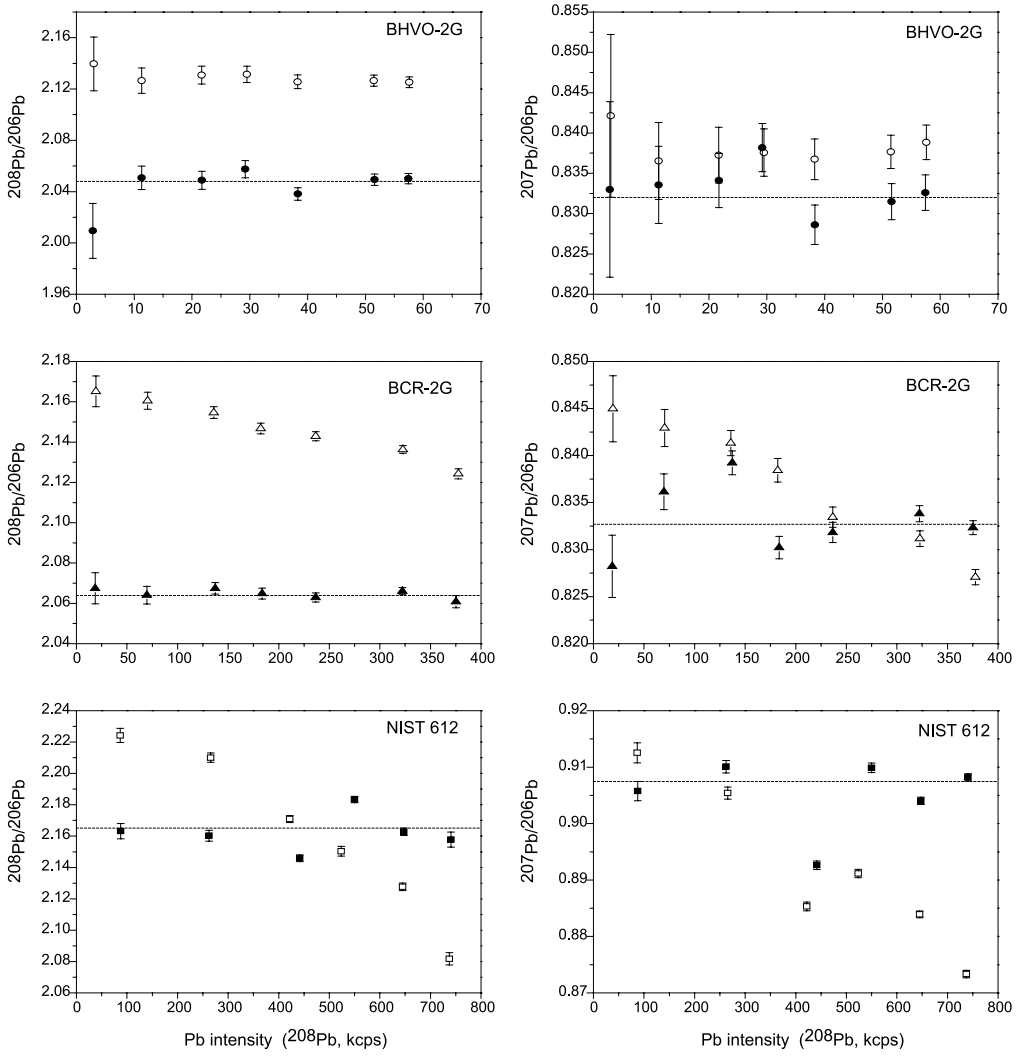

Fig. 3. Raw (open symbols) and corrected (solid symbols) $^{207,208}Pb/^{206}Pb$ ratios of BHVO-2G, BCR-2G, and NIST 612 measured at different ion beam intensities ranging from 3 to 750 kcps of ^{208}Pb. Beam intensity shown here is the unknown's, which is similar for bracketing standards also (see text). Error bars present independent in-run 2SE. Dashed lines show the reference values: Elburg et al. (2005) for BHVO-2G and BCR-2G, Baker et al. (2004) for NIST 612.

to set a suitable range of Pb ion intensities of bracketing standard and unknowns for the fsLA-MIC-ICP-MS system used, we measured Pb isotopic ratios and evaluated accuracy at different intensities of the ion beam. We also compared the isotopic ratios acquired from unmatched beam intensities between the unknowns and standards, because it was not always possible to perform intensity matching for samples such as small melt inclusions.

Figure 3 shows (1) raw $^{207,208}Pb/^{206}Pb$ ratios measured for BHVO-2G, BCR-2G, and NIST SRM 612, and (2) corrected $^{207,208}Pb/^{206}Pb$ ratios obtained by bracketing with the same sample at a laser repetition rate of 1–20 Hz, corresponding to ^{208}Pb intensity of 2.8–740 kcps. Pb intensity shown in Fig. 3 is the unknown's, but the corresponding bracketing standards also have similar beam intensity. Because the measurement at each laser repetition rate was done triply, which allowed a bracketing calibration by the sample itself for isotopic ratios, in order to examine the effects of beam intensity on accuracy of Pb isotopic determination by MICs.

The raw ratios were shifted systematically from the reference values and dropped significantly as the beam intensity increased (see open symbols in Fig. 3). The systematically low signal yield in IC2 for the ^{206}Pb ion beam explains the systematically high $^{207,208}Pb/^{206}Pb$ ratios in low ion beam regions. The $^{207,208}Pb/^{206}Pb$ ratios decreased continuously with increasing ion intensity (100–740 kcps at ^{208}Pb) for the BCR-2G and NIST SRM 612 glasses, suggesting more efficient signal yield in IC2 (^{206}Pb) in the high ion intensity range, or inversely, less efficient

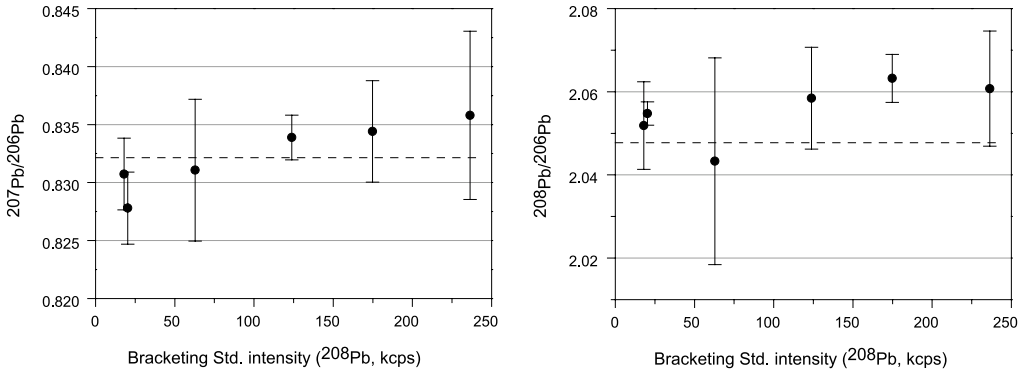

Fig. 4. $^{207,208}Pb/^{206}Pb$ ratios measured from ion beam intensity unmatched between unknown and standard. Shown is BHVO-2G with fixed beam intensity (^{208}Pb ~41 kcps) bracketed by BCR-2G at different beam intensities, and ^{208}Pb ranging from 18 to 236 kcps. The error bars are two standard deviations (2SD) in three individual measurements. The reference values of BHVO-2G (dashed lines) and BCR-2G Pb isotope data used in calculation are all from Elburg et al. (2005).

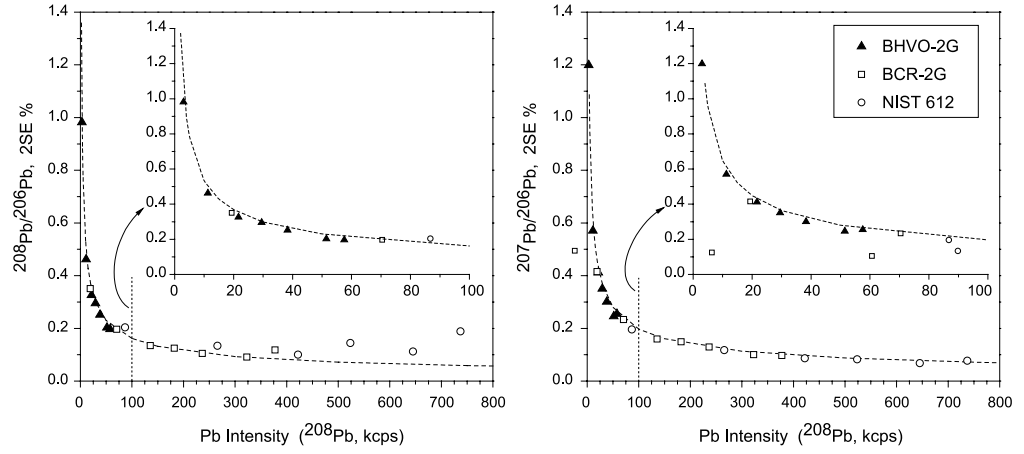

Fig. 5. Relative standard error (independent in-run 2SE%) versus beam intensity of ^{208}Pb isotopes. The signals were obtained by ablation on BHVO-2G, BCR-2G, and NIST 612 with 1–20 Hz laser repetition rate. The dashed lines show theoretical values.

signal yields in both IC3 (^{207}Pb) and IC4 (^{208}Pb) in the high intensity range. Such an effect was not significant in the low signal intensity range for the entire BHVO-2G results (<60 kcps at ^{208}Pb).

The internally corrected isotope ratios for all beam intensity levels replicated the reference isotope ratios closely (see solid symbols in Fig. 3), indicating the feasibility of using fsLA-MIC-ICP-MS for practical microanalysis of Pb isotopic ratios under the condition that bracketing standard and the unknown analyzed have similar signal intensities. The results also suggest: (1) that the standard bracketing method is useful for correcting for inter-MIC ion yield together with mass bias correction using exponential law (Albarède *et al*., 2004), and (2) that the miniature MICs are not stable internally with ion beams stronger than 300 kcps. For signal intensity level of 2.8–100 kcps of ^{208}Pb, all the isotope ratios measured in the three reference glasses were stable (Fig. 3). Such a low signal level should be suitable for Pb isotope analyses by this particular fsLA-MIC-ICP-MS method. However, data acquisition in a low signal level faces poor counting statistics. This will be examined in more detail below.

For further confirmation of this analytical protocol, we analyzed BHVO-2G (1.7 ppm Pb) as unknown at a fixed ^{208}Pb intensity of ~40 kcps using BCR-2G (11 ppm Pb) as bracketing standard with varying ^{208}Pb intensities of 30–250 kcps. The $^{206,207}Pb/^{206}Pb$ isotope ratios increased slightly (~0.5% of isotope ratios) with increasing intensity of the standard; however, these were within analytical uncertainty (2SD of 3 repeated analyses) (Fig. 4). The analyzed isotope ratios reproduced the reference values of BHVO-2G well (Elburg *et al*., 2005; see dotted lines in Fig. 4).

Note that a large instrumental mass bias (e.g., Hirata, 1996; Kent, 2008a; Kimura *et al*., 2013) in the Pb isotopes region was corrected for by the standard bracketing method (Elburg *et al*., 2005; Paul *et al*., 2005; Kent, 2008a; Kimura *et al*., 2013). The remaining interlinearity issue of the MICs can be well compensated in the 10–300 kcps range with the standard bracketing method.

Effect of Pb beam intensity on analytical precision

In-run precision of measured Pb isotope ratios from the above experiments showed an exponential correlation with ion beam intensity (proxy as ^{208}Pb intensity). The precision degraded dramatically when ^{208}Pb intensity decreased below 10 kcps (Fig. 5). An exception was the deterioration of precision of ^{208}Pb/^{206}Pb in the NIST SRM 612 glass when ^{208}Pb intensity >300 kcps. We concluded that this was caused by instantaneous saturations of IC4 by pulsed signals generated from coarse laser aerosol particles (e.g., Kimura *et al*., 2011).

Except for this, the observed precision agreed well with theoretical calculations, indicating that (1) the fsLA-MIC-ICP-MS analysis reached its limits of precision, (2) counting statistics were the main control of the analytical precision, and that (3) the background signals were properly subtracted from the signals. The typical background (gas blank) levels were 0.3–0.5 kcps at masses 206 and 207, and 1–1.5 kcps at mass 208 for carefully cleaned interface cones. The theoretical error calculations (see thin lines in Fig. 5) were performed as follows:

$$I^{20x\,\mathrm{Pb}} = I^{20x} - BG^{20x} \quad (x = 6,7,8)$$

$$\left(\sigma_{I^{20x\mathrm{Pb}}}\right)^2 = \left(\sigma_{I^{20x}}\right)^2 + \left(\sigma_{GB^{20x}}\right)^2$$

$$\sigma_{20i/206\,\mathrm{Pb}} = \frac{I^{20i\,\mathrm{Pb}}}{I^{206\,\mathrm{Pb}}} \times \sqrt{\left(\frac{\sigma^{20i\,\mathrm{Pb}}}{I^{20x\,\mathrm{Pb}}}\right)^2 + \left(\frac{\sigma^{206\,\mathrm{Pb}}}{I^{206\,\mathrm{Pb}}}\right)^2} \quad (i = 7,8)$$

$$SE_{20i/206\,\mathrm{Pb}} = \frac{\sigma_{20i/206\,\mathrm{Pb}}}{\sqrt{n}} \quad (i = 7,8),$$

where ^{20x}Pb is the intensity (cps) of the Pb ion beam, I is the intensity of the bulk ion beam; σ is the standard deviation of beam intensity or isotope ratios, SE is the standard error of the measured Pb isotope ratios, and n is total counting time. We assumed that the square root of a counting number represents one standard deviation following the counting statistics. Precisions calculated by this are given as 2SEs (or % 2SE), hereafter (Fig. 5).

Based on the equations and observed data above, we concluded that the optimal ion beam range with the miniature MICs is between 10 and 300 kcps at ^{208}Pb for sufficient counting statistics to allow in-run 2SE better than ~0.5%, but not to saturate the MICs in our fsLA-MIC-ICP-MS. Any signals from bracketing standards and bracketed unknowns should remain within the proposed range. This was achieved by altering the repetition rate of the fsLA pulse (1–10 Hz) for a ~30-μm crater using the rotation raster protocol.

Precision, accuracy and reproducibility of BHVO-2G analysis

We evaluated the fsLA-MIC-ICP-MS method for *in situ* Pb isotope analysis by an intensive measurement of BHVO-2G (1.7 ppm Pb), which had a Pb content equivalent to or lower than that of our target samples, including melt inclusions in olivine, which normally have one to a few tens of ppm Pb (e.g., Saal *et al*., 2005). The analysis also assessed Pb isotope ratios and isotopic homogeneity of BHVO-2G, for which few data have been published (Elburg *et al*., 2005; Jochum *et al*., 2005c). BCR-2G (11.0 ppm Pb) and NIST SRM 612 (38.96 ppm Pb) were used as bracketing standards.

Supplementary Table S2 and Fig. 6 present the results for BHVO-2G obtained in 14 analytical sessions over 15 months. All the measurements were conducted using ~30-μm crater by rotation raster and 10 Hz LA repetition rate, but the bracketing standard and plasma interface differed for each analytical session. Normal (N)-sample and X-skimmer cones were used for the first five days, whereas the JET-sample and X-skimmer cones were used for the remainder of the days for higher sensitivity, as shown in Table S2. Even with the JET-X cone combination, ^{208}Pb intensity of BHVO-2G ranged from 11 to 16 kcps after background subtraction. This was significantly lower than the previous report using MICs (using 40–67-μm crater by Sounders and Sylvester, 2008). The signal intensity can be increased by increasing the LA repetition rate while maintaining the horizontal resolution, but it results in an increased drilling depth. We did not apply an LA repetition rate greater than 10 Hz, to retain the total drilling depth <25 μm, to avoid exceeding the thickness of a typical rock thin section.

Even with such small Pb beam intensities, precisions of the Pb isotope ratios of BHVO-2G from individual craters were 0.5–1.4% (2SE) for ^{207}Pb/^{206}Pb and 0.4–1.0% (2SE) for ^{208}Pb/^{206}Pb (Table S2). The N-X cones yielded precisions of 0.7–1.4% (2SE) for ^{207}Pb/^{206}Pb and 0.6–1.0% (2SE) for ^{208}Pb/^{206}Pb, whereas those by JET-X cones performed better at 0.5–0.8% and 0.4–0.8% (2SE), respectively for these ratios (Table S2). The improvements were owing to the sensitivity being enhanced by three times when using the JET interface cone. It should be noted that the precisions (2SE) reported for BHVO-2G

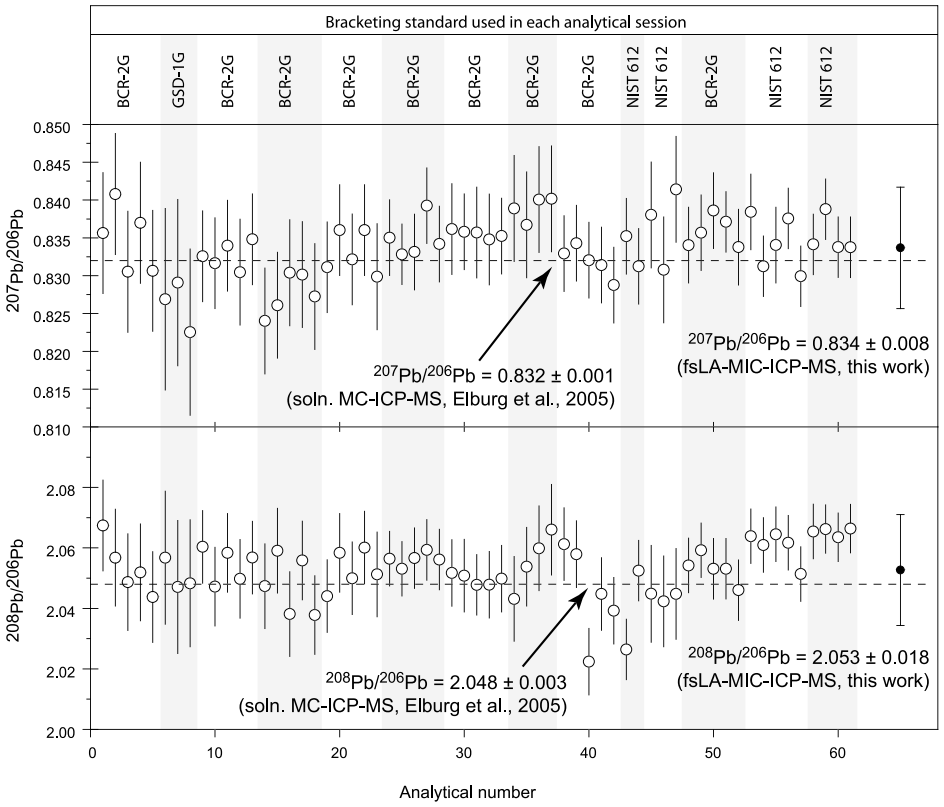

Fig. 6. Pb isotope ratios of BHVO-2G measured in 14 analytical sessions over 15 months by fsLA-MIC-ICP-MS using 30-μm crater of rotation raster and 10 Hz LA repetition rate. Error bar on each analysis (open symbol) is shown by bracketing standards propagated in-run 2SE. Solid symbol is the mean with error bar at 2SD of all sessions (n = 61). Dashed line represents reference values from solution MC-ICP-MS by Elburg et al. (2005).

and hereafter for other glasses were propagated from bracketing standards.

The mean values of measured $^{207}Pb/^{206}Pb$ and $^{208}Pb/^{206}Pb$ ratios were 0.834 ± 0.008 (2SD) and 2.053 ± 0.018 (2SD), respectively, which agree quite well with the solution MC-ICP-MS data (Elburg *et al*., 2005) to within 0.19% and 0.24%, respectively (Fig. 6). Our results were even closer to the LA-sector field (SF)-ICP-MS results by Jochum *et al*. (2005c), within 0.07% for the $^{207}Pb/^{206}Pb$ and <0.13% for the $^{208}Pb/^{206}Pb$ ratio. It should be noted, however, that about 25% of individual runs showed poorer accuracy and were scattered between 0.5% and 1.3% of accuracy for both isotope ratios. This was the worst analytical performance using this method, so far, although heterogeneity of the BHVO-2G glass may account for some of the scatter. Pb contamination of USGS standard seems a commonly believed issue (Baker *et al*., 2004; Elburg *et al*., 2005).

The measured $^{207}Pb/^{206}Pb$ and $^{208}Pb/^{206}Pb$ ratios showed overall reproducibility of 0.96% (2SD) and 0.89% (2SD), respectively (n = 61; Table S2). The reproducibility of both $^{207}Pb/^{206}Pb$ and $^{208}Pb/^{206}Pb$ were about twice that of the independent in-run precisions (about half size of propagated 2SE), implying large variety between different analytical sessions. We attributed this to the variation of the miniature MICs operating condition which was optimized for plateau voltages periodically but not in every analytical session. Pb isotopic heterogeneity of BHVO-2G may also have affected the long-term reproducibility because we analyzed different portions of the glass tip on different days.

fsLA-MIC-ICP-MS analyses of geological reference glasses

The long-term reproducibility obtained from BHVO-2G is encouraging for the application of this fsLA-MIC-ICP-MS method to natural glass samples, because most geological glass samples have higher Pb concentrations than BHVO-2G. In the following, we demonstrate the versatility of the method by analyzing MPI-DING (KL2-G basalt 2.07 ppm Pb, StHs6/80-G andesite 10.3 ppm Pb, ATHO-G rhyolite 5.67 ppm Pb, T1-G quartz diorite 11.6 ppm Pb, and GOR132-G komatiite 19.5 ppm Pb) and USGS (GSD-1G doped basalt, 48 ppm Pb) geological

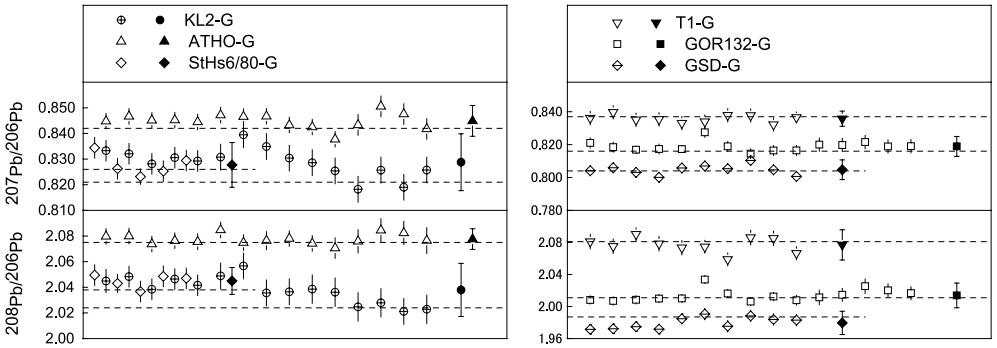

Fig. 7. $^{207,208}Pb/^{206}Pb$ ratios of KL2-G, StHs6/80-G, ATHO-G, T1-G, GOR132-G, and GSD-1G measured by fsLA-MIC-ICP-MS using 30-μm crater and variable LA repetition of 1–10 Hz. Error bar on each analysis (open symbol) is bracketing standards propagated in-run 2SE. Solid symbols represent mean value with error bars in 2SD. Dashed lines indicate the preferred values from Jochum et al. (2011).

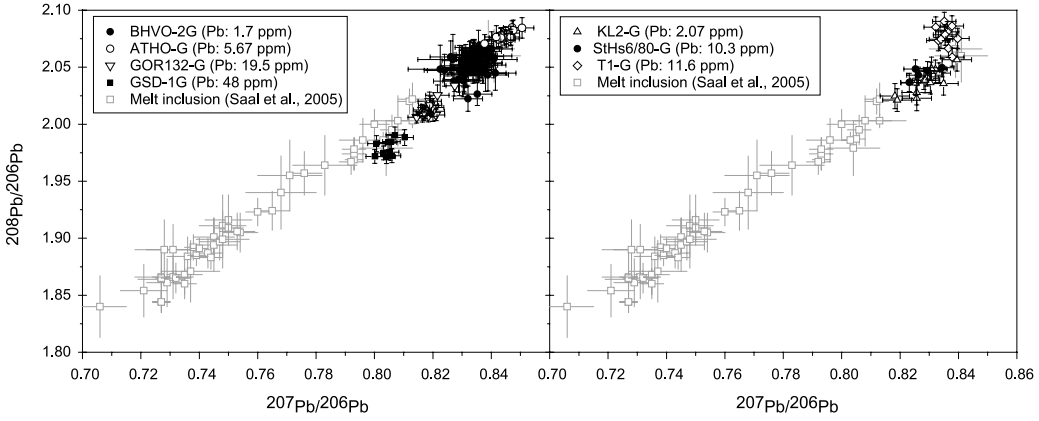

Fig. 8. Comparisons of Pb isotope analytical results on reference glasses by this work, together with those by SIMS on melt inclusions (Saal et al., 2005). Error bars with the data of this work are bracketing standards propagated in-run 2SE. Pb concentration data of the reference glasses are from Jochum et al. (2006), Guillong et al. (2005), and GeoReM (http://georem.mpch-mainz.gwdg.de, Application Ver. 15, 2013).

reference glasses covering almost the entire range of chemical compositions from komatiite, basalt, andesite, and rhyolite to quartz-diorite. These glasses have 2.07–19.5 ppm Pb, except for the doped basalt glass of GSD-1G, which contains 48 ppm Pb (Supplementary Table S3).

Figure 7 shows the $^{207}Pb/^{206}Pb$ and $^{208}Pb/^{206}Pb$ ratios of individual runs and mean values measured in this study for the MPI-DING and USGS glasses. Operating parameters of the fsLA-MIC-ICP-MS were the same as those used for BHVO-2G, but with varying LA repetition rates of 1–10 Hz depending on Pb abundance. Each glass was measured in two or more sessions, except for StHs6/80-G, which was analyzed only once. The JET-X cones were used for most analyses; except for a session in the GSD-1G analysis, which used N-X cones (Table S3). BCR-2G was used as standard for KL2-G, ATHO-G, and GOR132-G, whereas NIST SRM 612 was used for KL2-G, StHs6/80-G, ATHO-G, T1-G, and GOR132-G. Therefore, duplicate analyses were done by BCR-2G basalt and NIST SRM 612 synthetic (rhyolitic) glass standards with different matrices for KL2-G basalt, ATHO-G rhyolite, and GOR132-G komatiite to test various combinations of materials and matrix between the standard and sample.

The $^{207}Pb/^{206}Pb$ and $^{208}Pb/^{206}Pb$ measurements were all between 0.1% and 0.38% of the reference values (Jochum *et al.*, 2011) with reproducibility of 0.33–1.0% (2SD), except for KL2-G, which yielded an accuracy of 0.7–1% and reproducibility of 1–1.3% (Table S3 and Fig. 7). In general, the accuracy and precision accomplished from ~30 μm spatial resolution by fsLA-MIC-ICP-MS for these reference glasses were comparable to or better than those of BHVO-2G (see Table S2 and Fig. 6). The fsLA-MIC-ICP-MS method shown here was not affected by the matrix at the accuracy level of 0.1–0.38% for the

basalt, andesite, rhyolite, komatiite and quartz–diorite glasses. The relatively poor reproducibility of KL2-G may reflect its intrinsic heterogeneity. Sounders and Sylvester (2008) reported reproducibility of ~0.4% (2SD) and accuracy (<0.16%) of $^{207,208}Pb/^{206}Pb$ for KL2-G measured with LA-MC-ICP-MS using a 69-μm LA spot. This implies that Pb isotopic inhomogeneity may exist in KL2-G on a scale <69 μm. Alternatively, it may also reflect that some parts of KL2-G are homogeneous, but other parts are not.

Using a 30-μm crater and variable LA repetition rate of 1–10 Hz, ^{208}Pb beam intensity generated from these glasses ranged typically from 10 to 70 kcps. The independent in-run precisions at this Pb beam intensity were almost the same for all glasses, on average 0.28% (2SE) for $^{207}Pb/^{206}Pb$ and 0.19% (2SE) for $^{208}Pb/^{206}Pb$. These values were very close to those obtained by a solution MIC-ICP-MS with ^{208}Pb signal of ~200 kcps (Cocherie and Robert, 2007), indicating that our instrument, especially the 200-nm fsLA laser sampling system with rotation raster protocol, provided equally stable signals than that for solution nebulization (see Figs. 1 and 2). Careful tests on the appropriate signal range applied to the miniature MICs (see Figs. 3, 4, and 5) optimized the fsLA-MIC-ICP-MS.

The new analytical results of the selected geological glasses in this study were compared with the results on basalt melt inclusions analyzed by SIMS (Saal *et al*., 2005) (Fig. 8). The analyzed concentrations of Pb by SIMS were about several ppm, which are comparable with that analyzed for BHVO-2G (1.7 ppm Pb). The analytical precision (shown by 2SE for BHVO-2G) from an individual single crater was superior to the single spot precision by SIMS, whereas the reproducibility (shown by 2SD or deviation of the data cluster of BHVO-2G in Fig. 8) was similar to that of SIMS, and this was also true of other reference glasses (Fig. 8).

As such, analytical performance of the fsLA-MIC-ICP-MS system is comparable to SIMS apart from the poor depth resolution of 3–25 μm by the former, contrasting with the 2–5 μm by the latter. The spatial resolution accomplished by our fsLA-MIC-ICP-MS method is useful for the analyses of magmatic melt inclusions and silicate minerals where high resolution and sensitivity are required. The benefit of this method is its high throughput; it takes less than 400 seconds to measure an unknown sample in a typical arrangement of standard-sample bracketing. In contrast, 20–30 minutes are usually needed to perform Pb isotope analyses for one spot by SIMS (Kobayashi *et al*., 2004). The simple sample preparation without the necessity for either sample coating or insertion into high-vacuum conditions is an additional benefit. The cheaper set up costs and relatively easy availability of LA-ICP-MS over SIMS are also the advantages.

Conclusion

A simple and rapid *in situ* analytical method was established for high-resolution Pb isotope ratio analysis of geological glasses at low-Pb concentration. The system included a 200-nm fs laser ablation system for sampling at ~30-μm spatial resolution, and sensitivity-enhanced multiple ion counter (MIC)-ICP-MS. Optimization of the method by examining laser ablation protocols and responses of the miniature MICs helped identify the appropriate measurement conditions of the system. Intensive examinations on the geological reference glasses indicate comparable accuracy, precision and reproducibility of the $^{207,208}Pb/^{206}Pb$ ratios analyzed by the system to ion microprobe (e.g., SIMS). And besides, easy performance, high sample throughput and low cost are the most attractive points of the method for Pb isotopic studies of geological glasses, including melt inclusions in olivine.

Acknowledgments—We thank Dr. Y. Tatsumi of IFREE, JAMSETC (now at Kobe University) for generous support of this project. Thanks also go to Prof. K. P. Jochum of the Max Plank Institute for Chemistry for providing the MPI-DING glasses. Discussions with Dr. K. Shimizu of IFREE, JAMSETC are valuable. An anonymous reviewer and Dr. T. IIzuka are thanked for their constructive reviews of the manuscript. We also thank Prof. Martin Bizzarro for editorial handling and helpful comments. Technical and engineering support from Mr. K. Ohki of OK Laboratory Ltd. enabled the high transmission 200-nm fsLA optics to be constructed that helped establish the stable ablation.

References

Albarède, F., Telouk, P., Blichert-Toft, J., Boyet, M., Agranier, A. and Nelson, B. (2004) Precise and accurate isotopic measurements using multiple-collector ICPMS. *Geochim. Cosmochim. Acta* **68**, 2725–2744.

Baker, J., Peate, D., Waight, T. and Meyzen, C. (2004) Pb isotopic analysis of standards and samples using a ^{207}Pb–^{204}Pb double spike and thallium to correct for mass bias with a double-focusing MC-ICP-MS. *Chem. Geol.* **211**, 275–303.

Bouman, C., Deerberg, M., Schwieters, J. B. and Scientific, T. F. (2008) NEPTUNE and NEPTUNE Plus: Breakthrough in sensitivity using a large interface pump and new sample cone. *Application Note of Thermo Fischer Scientific* **30187**, 1–4.

Cocherie, A. and Robert, M. (2007) Direct measurement of lead isotope ratios in low concentration environmental samples by MC-ICP-MS and multi-ion counting. *Chem. Geol.* **243**, 90–104.

Czas, J., Jochum, K. P., Stoll, B., Weis, U., Yang, Q.-C., Jacob, D. E. and Andreae, M. O. (2012) Investigation of matrix effects in 193 nm laser ablation-inductively coupled plasma-mass spectrometry analysis using reference glasses of different transparencies. *Spectrochim. Acta Part B* **78**, 20–28.

Elburg, M., Vroon, P., Wagt, B. and Tchalikian, A. (2005) Sr

and Pb isotopic composition of five USGS glasses (BHVO-2G, BIR-1G, BCR-2G, TB-1G, NKT-1G). *Chem. Geol.* **223**, 196–207.

Gagnevin, D., Daly, J. S., Waight, T. E., Morgan, D. and Poli, G. (2005) Pb isotopic zoning of K-feldspar megacrysts determined by Laser Ablation Multi-Collector ICP-MS: Insights into granite petrogenesis. *Geochim. Cosmochim. Acta* **69**, 5171–5171.

GeoReM (2013) Application Ver. 15, Available at http://georem.mpch-mainz.gwdg.de

Guillong, M., Hametner, K., Reusser, E., Wilson, S. A. and Günther, D. (2005) Preliminary characterisation of new glass reference materials (GSA-1G, GSC-1G, GSD-1G and GSE-1G) by laser ablation-inductively coupled plasma-mass spectrometry using 193 nm, 213 nm and 266 nm wavelengths. *Geostand. Geoanal. Res.* **29**, 315–331.

Hirata, T. (1996) Lead isotopic analyses of NIST standard reference materials using multiple collector inductively coupled plasma mass spectrometry coupled with a modified external correction method of mass discrimination effect. *Analyst* **121**, 1407–1411.

Jochum, K. P., Nohl, U., Herwig, K., Lammel, E., Stoll, B. and Hofmann, A. W. (2005a) GeoReM: A New geochemical database for reference materials and isotopic standards. *Geostand. Geoanal. Res.* **29**, 333–338.

Jochum, K. P., Pfänder, J., Woodhead, J. D., Willbold, M., Stoll, B., Herwig, K., Amini, M., Abouchami, W. and Hofmann, A. W. (2005b) MPI-DING glasses: New geological reference materials for *in situ* Pb isotope analysis. *Geochem. Geophys. Geosys.* **6**, Q10008.

Jochum, K. P., Stoll, B., Herwig, K., Amini, M., Abouchami, W. and Hofmann, A. W. (2005c) Lead isotope ratio measurements in geological glasses by laser ablation-sector field-ICP mass spectrometry (LA-SF-ICP-MS). *Int. J. Mass Spectrom.* **242**, 281–289.

Jochum, K. P., Stoll, B., Herwig, K., Willbold, M., Hofmann, A. W., Amini, M., Aarburg, S., Abouchami, W., Hellebrand, E., Mocek, B., Raczek, I., Stracke, A., Alard, O., Bouman, C., Becker, St., Dücking, M., Brätz, H., Klemd, R., de Bruin, D., Canil, D., Cornell, D., de Hoog, J. C. M., Dalpé, C., Danyushevsky, L. V., Eisenhauer, A., Gao, Y., Snow, J. E., Groschopf, N., Günther, D., Latkoczy, C., Guillong, M., Hauri, E., Höfer, H. E., Lahaye, Y., Horz, K., Jacob, D. E., Kasemann, S., Kent, A. J. R., Zack, T., Ludwig, T., Mason, P. R. D., Meixner, A., Rosner, M., Misawa, K., Nash, B. P., Pfänder, J. A., Premo, W. R., Sun, W. D., Tiepolo, M., Vannucci, R., Vennemann, T., Wayne, D. and Woodhead, J. D. (2006) MPI-DING reference glasses for *in situ* microanalysis: New reference values for element concentrations and isotope ratios. *Geochem. Geophys. Geosys.* **7**, Q02008.

Jochum, K. P., Wilson, S. A., Abouchami, W., Amini, M., Chmeleff, J., Eisenhauer, A., Hegner, E., Iaccheri, L. M., Kieffer, B., Krause, J., McDonough. W. F., Mertz-Kraus, R., Raczek, I., Rudnick, R. L., Scholz, D., Steinhoefel, G., Stoll, B., Stracke, A., Tonarini, S., Weis, D., Weis, U. and Woodhead, J. D. (2011) GSD-1G and MPI-DING reference glasses for *in situ* and bulk isotopic determination. *Geostand. Geoanal. Res.* **35**, 193–226.

Kent, A. J. R. (2008a) *In-situ* analysis of Pb isotope ratios using laser ablation MC-ICP-MS: Controls on precision and accuracy and comparison between Faraday cup and ion counting systems. *J. Anal. Atom. Spectrom.* **23**, 968–975.

Kent, A. J. R. (2008b) Lead isotope homogeneity of NIST SRM 610 and 612 glass reference materials: Constraints from laser ablation multicollector ICP-MS (LA-MC-ICP-MS) analysis. *Geostand. Geoanal. Res.* **32**, 129–147.

Kent, A. J. R. and Dilles, J. H. (2005) *In-situ* analysis of Pb isotope ratios by LA-MC-ICP-MS: Applications to ore genesis and igneous petrogenesis. *Geochim. Cosmochim. Acta* **69**, A376–A376.

Kimura, J.-I. and Chang, Q. (2012) Origin of the suppressed matrix effect for improved analytical performance in determination of major and trace elements in anhydrous silicate samples using 200 nm femtosecond laser ablation sector-field inductively coupled plasma mass spectrometry. *J. Anal. Atom. Spectrom.* **27**, 1549–1559.

Kimura, J.-I., Chang, Q. and Tani, K. (2011) Optimization of ablation protocol for 200 nm UV femtosecond laser in precise U–Pb age dating coupled to multi-collector ICP mass spectrometry. *Geochem. J.* **45**, 283–296.

Kimura, J.-I., Kawabata, H., Chang, Q., Miyazaki, T. and Hanyu, T. (2103) Pb isotope analyses of silicate rocks and minerals with Faraday detectors using enhanced-sensitivity laser ablation-multiple collector-inductively coupled plasma mass spectrometry. *Geochem. J.* **47**, 369–384.

Kobayashi, K., Tanaka, R., Moriguti, T., Shimizu, K. and Nakamura, E. (2004) Lithium, boron, and lead isotope systematics of glass inclusions in olivines from Hawaiian lavas: evidence for recycled components in the Hawaiian plume. *Chem. Geol.* **212**, 143–161.

Mathez, E. A. and Waight, T. E. (2003) Lead isotopic disequilibrium between sulfide and plagioclase in the Bushveld Complex and the chemical evolution of large layered intrusions. *Geochim. Cosmochim. Acta* **67**, 1875–1888.

Nozaki, T., Suzuki, K., Ravizza, G. E., Kimura, J.-I. and Chang, Q. (2012) A method for rapid determination of Re and Os isotope compositions using ID-MC-ICP-MS combined with the sparging method. *Geostand. Geoanal. Res.* **36**, 131–148.

Paul, B., Woodhead, J. D. and Hergt, J. (2005) Improved *in situ* isotope analysis of low-Pb materials using LA-MC-ICP-MS with parallel ion counter and Faraday detection. *J. Anal. Atom. Spectrom.* **20**, 1350–1357.

Paul, B., Woodhead, J. D., Hergt, J., Danyushevsky, L., Kunihiro, T. and Nakamura, E. (2011) Melt inclusion Pb isotope analysis by LA-MC-ICPMS: Assessment of analytical performance and application to OIB genesis. *Chem. Geol.* **289**, 210–223.

Pearce, N. J. G., Perkins, W. T., Westgate, J. A., Gorton, M. P., Jackson, S. E., Neal, C. R. and Chenery, S. P. (1997) A compilation of new and published major and trace element data for NIST SRM 610 and NIST SRM 612 glass reference materials. *Geostand. Newslett.* **21**, 115–144.

Peate, I. U., Baker, J. A., Kent, A. J. R., Al-Kadasi, M., Al-Subbary, A., Ayalew, D. and Menzies, M. (2003) Correlation of Indian Ocean tephra to individual Oligocene silicic eruptions from Afro-Arabian flood volcanism. *Earth Planet. Sci. Lett.* **211**, 311–327.

Saal, A. E., Hart, S. R., Shimizu, N., Hauri, E. H., Layne, G. D. and Eiler, J. M. (2005) Pb isotopic variability in melt inclusions from the EMI-EMII-HIMU mantle end-members and the role of the oceanic lithosphere. *Earth Planet. Sci. Lett.* **240**, 605–620.

Simon, J. I., Reid, M. R. and Young, E. D. (2007) Lead isotopes by LA-MC-ICPMS: Tracking the emergence of mantle signatures in an evolving silicic magma system. *Geochim. Cosmochim. Acta* **71**, 2014–2035.

Souders, A. K. and Sylvester, P. J. (2008) *Laser Ablation ICP-MS in the Earth Sciences: Current Practices and Outstanding Issues*, Vol. 50 (Sylvester, P. J., ed.), 265–282, Mineralogical Association of Canada, Vancouver, BC.

Westgate, J. A., Pearce, N. J. G., Perkins, W. T., Shane, P. A. and Preece, S. J. (2011) Lead isotope ratios of volcanic glass by laser ablation inductively-coupled plasma mass spectrometry: Application to Miocene tephra beds in Montana, USA and adjacent areas. *Quatern. Int.* **246**, 82–96.

Supplementary Materials

URL (http://www.terrapub.co.jp/journals/GJ/archives/data/48/MS307.pdf)
Tables S1 to S3